



HAL
open science

Acousto-optic interaction in 2D LiNbO₃ phoxonic crystal

Quentin Rolland, Samuel Dupont, Joseph Gazalet, Jean-Claude Kastelik, Yan Penneç

► **To cite this version:**

Quentin Rolland, Samuel Dupont, Joseph Gazalet, Jean-Claude Kastelik, Yan Penneç. Acousto-optic interaction in 2D LiNbO₃ phoxonic crystal. Acoustics 2012, Apr 2012, Nantes, France. paper 000490, 3403-3408. hal-00801108

HAL Id: hal-00801108

<https://hal.science/hal-00801108>

Submitted on 15 Mar 2013

HAL is a multi-disciplinary open access archive for the deposit and dissemination of scientific research documents, whether they are published or not. The documents may come from teaching and research institutions in France or abroad, or from public or private research centers.

L'archive ouverte pluridisciplinaire **HAL**, est destinée au dépôt et à la diffusion de documents scientifiques de niveau recherche, publiés ou non, émanant des établissements d'enseignement et de recherche français ou étrangers, des laboratoires publics ou privés.



ACOUSTICS 2012

Acousto-optic interaction in 2D LiNbO₃ phoxonic crystal

Q. Rolland, S. Dupont, J. Gazalet, J.-C. Kastelik and Y. Pennec

IEMN, UVHC, IEMN UMR 8520, F-59313 Valenciennes, France
quentin.rolland@univ-valenciennes.fr

Recently, the possibility to create simultaneously a photonic and phononic crystal has been demonstrated. Those structures are referred to as “phoxonic” crystals, they consist in arrays of holes drilled in a matrix. Fundamental research actions aims at studying acoustic and electromagnetic waves propagation in these structures in order to find simultaneous band gaps, then finding out confined modes in defect (cavity or waveguides). Phoxonic crystals are expected to enhance the acousto-optic interaction thanks to the localization of both waves in the same defect.

We investigate in this paper the potential benefits of an acousto-optic interaction in LiNbO₃ phoxonic crystals. We model 2D phoxonic crystals using Finite Element Method. A first work consists in finding out the most suitable filling factor and lattice parameter so as to have simultaneous band gaps. Afterwards we discuss how the electromagnetic wave is affected by elasto-optic and electro-optic effects. The results show an increased sensitivity of optical cavity defect modes frequencies caused by the strong confinement of both waves in the defect.

1 Introduction

Photonic and Phononic crystals have both caught attention of many research groups during the last two decades [1-6]. These structures, consists in periodic inclusions of holes drilled on a substrate. They offer new ways to control sound and light at the same time. In particular, periodic structures having sizes comparable to the sound and light wavelength exhibits ranges of frequencies that forbid the propagation of both waves. If these waves can not propagate in any direction, the structures exhibits complete band gap, the so-called forbidden band.

Numerous studies on 2D periodic structures have been dedicated to the search of complete band gap, especially for simultaneous electromagnetic and acoustic complete band gaps. For instance, Moldovan and Thomas [1,2] have shown theoretically that photonic and phononic complete band gap can be easily obtained on periodic air holes drilled on a matrix made of Silicon. Further work [4-5] has been achieved using different periodic structures, such as square, hexagonal or honeycomb structures and their impact on the complete band gap has been studied. Other works examine the influence of other parameters of the crystals on simultaneous band gap. D. Bria et al [3] studied the impact of different filling factors on both photonic and phononic band gaps. Said Sadat- Saleh et al [4] studied the band gap variations depending on different holes sizes in a unit cell.

Interesting phenomena arises from the interaction of light and sound in periodic structures. Indeed, the acoustic wave induces perturbations of the optical properties of these structures. We investigate optical acoustical couplings based on three different effects.

We consider first the photo-elastic effect [7], the so-called Pockels effect: the acoustic strain induces a change of the refractive index spatial distribution in the crystal. Refractive index modifications affect the optical wave propagation.

Secondly, for piezoelectric materials, electro-optic effect has to be taken into account as well [7], due to the electric field accompanying the acoustical wave. It modifies in a similar way the refractive index of the phoxonic crystal materials.

Finally, the acoustically induced displacement, modifies the phoxonic crystal geometry, this effect is referred to as opto-mechanical effect [6]. Likewise, it leads to perturbations of the electromagnetic wave propagation.

In this paper, we focus our attention on defects for which an inclusion or an array of inclusions has been removed from the crystal, leading to the creation of a cavity or a waveguide. Indeed, structures possessing such defects allow confining both acoustic and optical wave energy. Many papers have been devoted to simultaneous localization of both phonon and photon [2,8-9]. We will investigate in the present paper the spatial distribution of cavity modes and explore the possibility to improve acousto-optic interaction.

The main objective of this paper is to study the acousto-optic couplings effects in 2D phoxonic crystal with circular inclusions. The investigations are focused on lithium niobate (LiNbO₃) substrate in view of exploiting its strong acousto-optical and piezoelectric coefficients. The thickness of the crystal is assumed to be infinite allowing us to perform 2D calculation. The computation has been carried out on YX-cut [10-11].

The paper is structured as follow: first we consider the different key parameters involved in the phoxonic crystal design, the impact of the radius of the air inclusion, depending on the different structures is investigated. Then we study the different cavity modes of a defect added in the periodic structure. Finally, we describe the different acousto-optic related effects and the main results obtained.

2 Photons and phonons complete band-gaps

To show the existence of localized modes, the presence of band gaps needs first to be studied. In particular, it is required to design a structure possessing both acoustic and optical complete band gaps in order to obtain simultaneous light and sound localization. Regarding the crystal, a judicious choice of parameters is needed to obtain the simultaneous gaps and hence the likelihood to promote the simultaneous localization of photons and phonons. We focus our attention on the effect of different inclusions radius and different types of structure on the complete band gaps.

Band structures are computed for a crystal lattice made up of lithium niobate. Assuming an infinite and periodic structure in the (x,y) axis, we use Bloch-Floquet function as periodic boundary condition at each side of the unit cell in order to reduce the domain of calculation. All the results are based on Finite Element Method (FEM) computations

on a unit cell. Figures 1-3 shows on the bottom left part the reduced Brillouin zone needed to compute band diagrams, the corresponding structure is illustrated on the top left part of the figures. Since elastic wave can not propagate in vacuum, only solid materials is meshed for phononic crystals while all domains are meshed for photonic crystals. Considering a 2D plane, elastic waves are composed of mixed modes consisting of coupled shear and longitudinal waves in x - y planes (in-plane). In this model, no shear vibration along the z -axis (out-of-plane) is taken into account.

In view of the technological realization of integrated structures for electronic and telecommunication based devices, we consider the optical modes in the range of telecommunication wavelength with the acoustic frequencies falling in the gigahertz range. As the wavelength of both acoustic and optical wave must be in the same range and comparable to the lattice constant, we choose a lattice parameter a around 650 nm for the following results.

The computed results on figures 1-3 shows the evolution of complete band gaps, using honeycomb, triangular and square structures respectively as a function of the normalized radius varying from 0,25 up to 0,49. We denote r the radius of the circular inclusion and a the lattice parameter. Complete band gaps are presented using normalized frequency for phononic crystal in blue on the top part of figures, and for photonic crystal on the bottom part of figures. We consider the TE polarized mode (out-of-plane electric field) and the TM polarized mode (in-plane electric field) in red and in green respectively. We denote ω the angular frequency and c the velocity of the optical wave.

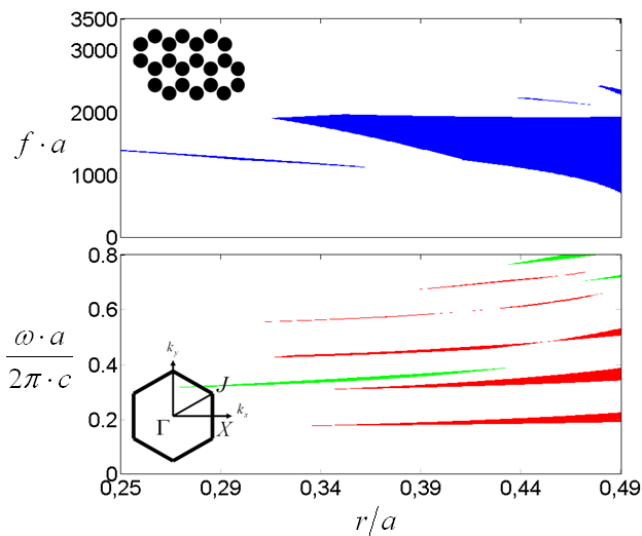


Figure 1: Band-gap evolution as a function of normalized radius of *honeycomb* structure for phononic crystal (top part) and photonic crystal (bottom part)

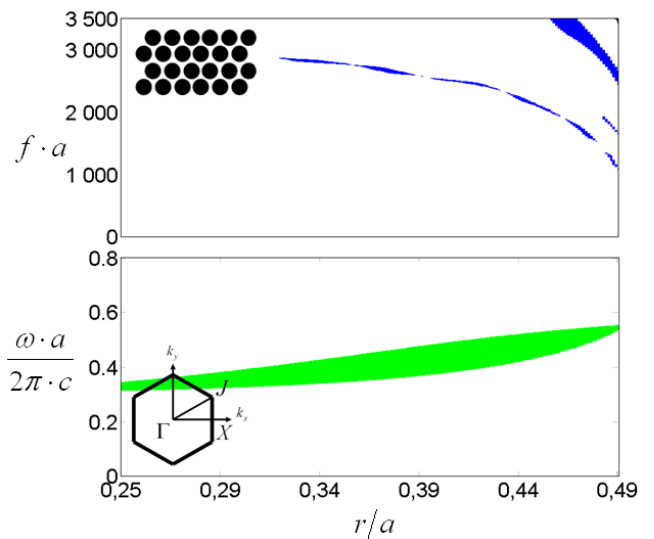


Figure 2: Band-gap evolution as a function of normalized radius of *triangular* structure for phononic crystal (top part) and photonic crystal (bottom part)

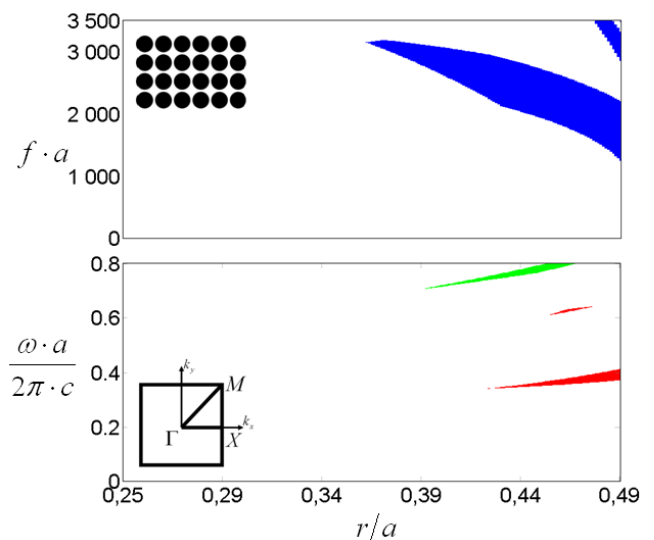


Figure 3: Band-gap evolution as a function of normalized radius of *square* structure for phononic crystal (top part) and photonic crystal (bottom part)

The computed results for the three different structures shows wide acoustic band gaps for square and honeycomb structures compared with triangular structure. We observe that high values for the normalized radius is privileged for wider band gap. However results for photonic crystal show in general thinner band gaps. Triangular based structures have a larger gap, especially for TM mode, than other structures while square based structures have much less widespread gaps. Computed results for 2D phoxonic crystal made up of LiNbO_3 are consistent with the literature [4-5].

In order to increase the likelihood to obtain simultaneous localization of photon and phonon, choosing the honeycomb structure appears to be the appropriate choice. Indeed, only sufficient acoustics gaps are available for square and honeycomb lattice, and the latter offers the most widespread optical gaps. Concerning the normalized radius, a compromise must be reached between photonic and phononic band gap. We consider that $r/a = 0.43$ is good candidate. As a consequence, using the lattice parameter value, we use $r = 280$ nm.

3 Photons and Phonons confinement in defects

The effect of introducing a cavity within the structure is studied in an attempt to localize acoustic and electromagnetic modes. For the purpose of reducing the calculation domain, supercell computations were performed to investigate cavity modes by removing an inclusion in its center. We choose to compute a 6x6 supercell using Bloch-Floquet periodic conditions at each side of the domain. In a similar way, periodic air holes are not meshed for phononic crystals while all domains are meshed for photonic crystals. The corresponding unit cell of a honeycomb, as opposed to square and triangular unit cells, includes two identical holes. In order to promote the simultaneous localization of photons and phonons, instead of an entire unit cell, only an inclusion has been removed.

Figure 4 shows the band diagram for acoustic supercell on the left part of the figure. Optical band diagrams are displayed as well on figures 5-6 for TE and TM polarized modes on the left part. For sake of simplicity, only eigenfrequencies along the ΓX direction according to the irreducible Brillouin zone were computed. We observe the band folding phenomena in supercell band diagrams. Black dotted lines represent the edges of band gaps computed with a unit cell. We can notice a direct match between the band gap computed with a supercell and unit cell. However further additional modes, located inside or close to the band gap edges, appear. Those modes correspond to cavity modes, illustrated on the right side of the figures.

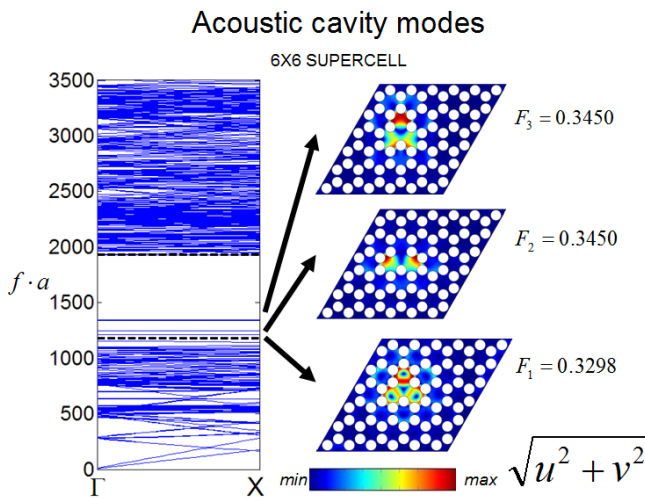


Figure 4: 6x6 Supercell band diagrams along ΓX direction for honeycomb phononic crystal with a point defect and their corresponding cavity modes field distribution of acoustic displacement

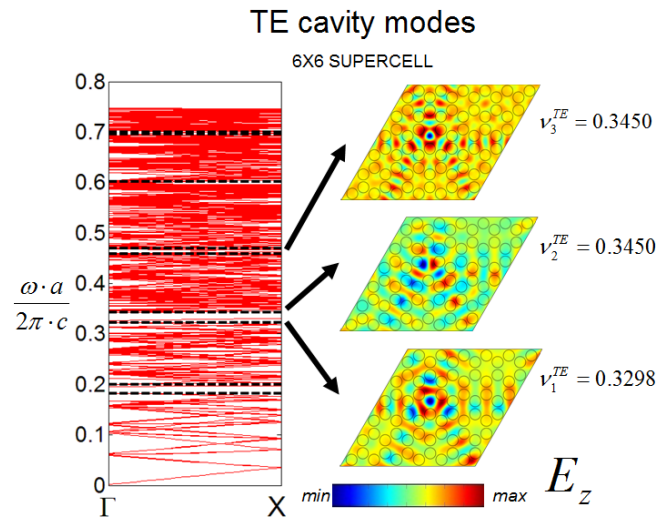


Figure 5: 6x6 Supercell band diagrams along ΓX direction for honeycomb photonic crystal with a point defect and their corresponding cavity modes electric field distribution

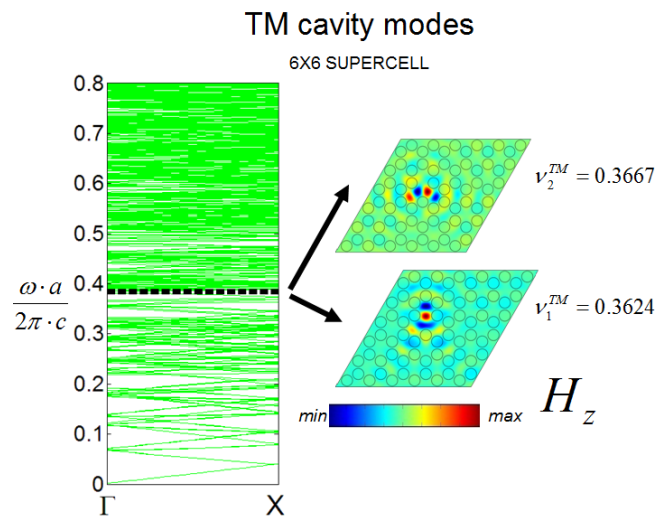


Figure 6 : 6x6 Supercell band diagrams along ΓX direction for honeycomb photonic crystal with a point defect and their corresponding cavity modes magnetic field distribution

To illustrate the localization of photons and phonons, figures 4-6 displays the field distribution of the cavity modes. Figure 4 shows the magnitude of the in-plane total displacement $|u_i|$, figures 5 and 6 shows the magnitude of the out-of-plane electric field E_z and magnetic field H_z respectively. Cavity modes field distributions show clearly photons and phonons confinement in the defect. Amongst all modes computed, those represented are the most significant ones.

We observe cavity modes which increase confinement of photons and phonons. As the confinement degree of photons and phonons yields a higher energy confinement, appropriate acoustic and optical modes must be chosen to promote a better acousto-optic interaction. At the same time, modes sharing similar distribution profiles are more likely to increase the acousto-optic effect. Here we choose to use F_2 and v_2^{TM} for the following results.

4 Acousto-optic interaction

As mentioned earlier, acoustical and optical coupling phenomenon in periodic structures induce a perturbation of the electromagnetic field thanks to three different mechanisms [6-7]. We consider first the Pockels effect given by (1):

$$\Delta\eta_{ij}^{pE} = p_{ijkl}S_{kl} \quad (1)$$

where p_{ijkl} is the photo-elastic constants of the media and S_{kl} the acoustic strain. Any deformation S_{kl} will lead to the modification of $\Delta\eta_{ij}$, η_{ij} being the impermeability tensor. The latter represents the inverse of the permittivity tensor ε_{ij} given by (2):

$$\varepsilon_{ij} \cdot \eta_{jk} = \delta_{ik} \quad (2)$$

Due to the piezoelectric property of lithium niobate, the acoustic electric field E_p affects in a similar way the impermeability tensor through the electro-optic effect represented by tensor r_{ijp} . We use in the following relation to compute the electro-optic contribution (3):

$$\Delta\eta_{ij}^{eO} = r_{ijp}E_p \quad (3)$$

Finally, the opto-mechanical effect results from the structure geometry deformation. In particular, the boundaries displacement of each inclusion of the substrate:

$$\begin{aligned} \Delta x(t) &= x(t) + x_o \\ \Delta y(t) &= y(t) + y_o \end{aligned} \quad (4)$$

Considering the propagation of both acoustic and optical wave in the (x,y) plane, and the lithium niobate crystal symmetry equation (1) reduces to:

$$\begin{aligned} \Delta\varepsilon_{11}^{pE} &= -\varepsilon_o^2(S_1p_{11} + S_2p_{22}) \\ \Delta\varepsilon_{22}^{pE} &= -\varepsilon_e^2(S_1p_{12} + S_2p_{11}) \\ \Delta\varepsilon_{33}^{pE} &= -\varepsilon_o^2p_{31}(S_1 + S_2) \\ \Delta\varepsilon_{12}^{pE} &= \Delta\varepsilon_{21}^{pE} = -S_6\varepsilon_o\varepsilon_e \frac{p_{11} + p_{12}}{2} \\ \Delta\varepsilon_{13}^{pE} &= \Delta\varepsilon_{31}^{pE} = -S_6\varepsilon_o^2p_{41} \\ \Delta\varepsilon_{23}^{pE} &= \Delta\varepsilon_{32}^{pE} = -\varepsilon_o\varepsilon_e p_{41}(S_1 - S_2) \end{aligned} \quad (5)$$

In a similar way, equation (3) can be rewritten as:

$$\begin{aligned} \Delta\varepsilon_{11}^{eO} &= E_y\varepsilon_o^2r_{22} \\ \Delta\varepsilon_{22}^{eO} &= -E_y\varepsilon_e^2r_{22} \\ \Delta\varepsilon_{33}^{eO} &= 0 \\ \Delta\varepsilon_{12}^{eO} &= \Delta\varepsilon_{21}^{eO} = E_x\varepsilon_e\varepsilon_o r_{22} \\ \Delta\varepsilon_{13}^{eO} &= \Delta\varepsilon_{31}^{eO} = -E_x\varepsilon_o^2r_{42} \\ \Delta\varepsilon_{23}^{eO} &= \Delta\varepsilon_{32}^{eO} = -E_y\varepsilon_e\varepsilon_o r_{42} \end{aligned} \quad (6)$$

$\Delta\varepsilon_{ij}^{pE}$ and $\Delta\varepsilon_{ij}^{eO}$ denotes for the relative permittivity variation of the photo-elastic and electro-optic effect. ε_o and ε_e represents the ordinary and extraordinary relative permittivity respectively.

To be closer to reality, we consider a maximum input acoustic strain of 10^{-3} [6]. As a consequence, the generated acoustic displacement does not exceed $u_{inc} = a \cdot 10^{-3}/3$. The computed displacements inside the cavity show that the amplitude of acoustical displacement can be as high as 30 times compared to the incident wave.

According to (1) and (3) the relative permittivity spatial variation is related to the acoustic wave. The related effects thus show a time varying permittivity variation depending on the acoustic frequency. To illustrate the impact of acousto-optic coupling phenomena based on these three effects, we focus our attention on the cavity mode resonant wavelength. Indeed, the acoustic wave induces a change of the spatial distribution of refractive index Δn_{ij} deduced from $\Delta\varepsilon_{ij}^{pE}$ and $\Delta\varepsilon_{ij}^{eO}$. As a consequence, the optical cavity modes are modified. Their corresponding resonant frequencies ν_i are modified depending on the different effects. We deduce from $\Delta\nu_i$ the change of the optical wavelength $\Delta\lambda_i$.

Figure 7 displays the normalized wavelength of $\Delta\lambda_2^{TM}$ as a function of $\Omega \cdot t$ varying from 0 up to $2 \cdot \pi$. The green line represents the wavelength modulation based on the photo-elastic effect, the blue line represents the electro-optic effect and the black line the opto-mechanical effect. We notice that results give close values around $1.5 \cdot 10^{-3}$ which is consistent with reported values for 2D crystal [12].

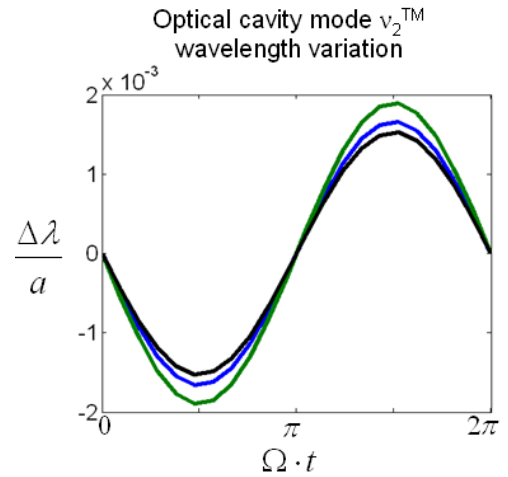


Figure 7: cavity resonant wavelength variation as a function of acoustic angular frequency, according to photo-elastic effect (green line), electro-optic effect (blue line) and opto-mechanical effect.

A similar simulation has been completed using a different optical mode. Results show that the spread of optical wavelength variation can be significant. As a consequence, the choice of acoustic and optical cavity modes has a strong impact on the acousto-optic interaction.

5 Conclusion

We have presented the study of a two dimensions phoxonic structure on Lithium Niobate. Band diagrams for acoustic and optical waves are computed with 2D FEM models. The impact of acoustic wave on photonic cavity modes due to photo-elastic, electro-optic and opto-mechanic effects has been evaluated. From the simulation results, optical cavity modes resonant frequencies can show a relative shift in the order of 10^{-3} .

Acknowledgments

This work has been carried out within the phoXcry project n°ANR-09-NANO-004 funded by the French National Agency (ANR) in the frame of its 2009 programme in Nanosciences, Nanotechnologies and Nanosystems (P3N2009).

References

- [1]. M. Maldovan and E.L. Thomas, "Simultaneous complete elastic and electromagnetic band gaps in periodic structures", *Appl. Phys. B* **83**, 595–600 (2006)
- [2]. M. Maldovana and E.L. Thomas, "Simultaneous localization of photons and phonons in two-dimensional periodic structures", *Appl. Phys. Lett.* **88**, 251907 (2006)
- [3]. D. Bria, M. B. Assouar, M. Oudich, Y. Pennec, J. Vasseur, and B. Djafari-Rouhani, "Opening of simultaneous photonic and phononic band gap in two-dimensional square lattice periodic structure", *J. of Appl. Phys.* **109**, 014507 (2011)
- [4]. S. Sadat-Saleh, S. Benchabane, F.I. Baida, M-P. Bernal, and V. Laude, "Simultaneous photonic and phononic band gaps in a two-dimensional lithium niobate crystal", *IEEE 10.1109 / ULTSYM.2009.0269* (2009)
- [5]. S. Sadat-Saleh, S. Benchabane, F.I. Baida, M-P. Bernal, and V. Laude, "Tailoring simultaneous photonic and phononic band gaps", *J. of Appl. Phys.* **106**, 074912 (2009)
- [6]. E. Psarobas, N. Papanikolaou, N. Stefanou, B. Djafari-Rouhani, B. Bonello, V. Laude, "Enhanced acousto-optic interactions in a one-dimensional phoxonic cavity", *Phys. Rev. B* **82**, 174303 (2010)
- [7]. D. Royer, E. Dieulesaint "Elastic Waves in solids II - Royer, Dieulesaint", *Springer (1999)*
- [8]. Y. Pennec, B. Djafari Rouhani, C. Li, J. M. Escalante, A. Martinez et al. "Band gaps and cavity modes in dual phononic and photonic strip waveguides", *AIP* **1**, 041901 (2011)
- [9]. V. Laude, J-C. Beugnot, S. Benchabane, Y. Pennec, B. Djafari-Rouhani, N. Papanikolaou, J.M. Escalante, and A. Martinez, "Simultaneous guidance of slow photons and slow acoustic phonons in silicon phoxonic crystal slabs", *OPTICS EXPRESS* 9690 / 9 May 2011 / Vol. 19, No. 10
- [10]. V. Laude, M. Wilm, S. Benchabane, and A. Khelif "Full band gap for surface acoustic waves in a piezoelectric phononic crystal", *Phys. Rev. E* **71**, 036607 (2005)
- [11]. D. Yudistira, Y. Pennec, B. Djafari Rouhani, S. Dupont, and V. Laude "Non-radiative complete surface acoustic wave bandgap for finite-depth holey phononic crystal in lithium niobate", *Appl. Phys. Lett.* **100**, 061912 (2012)
- [12]. D. A. Fuhrmann, S. M. Thon, H. Kim, D. Bouwmeester, P. M. Petroff, A. W. and H. J. Krenner "Dynamic modulation of photonic crystal nanocavities using gigahertz acoustic phonons", *NATURE PHOTONICS | VOL 5 | OCTOBER 2011*